

Vacuum-Ultraviolet (VUV) Photoionization of Small Methanol and Methanol–Water Clusters[†]

Oleg Kostko, Leonid Belau, Kevin R. Wilson, and Musahid Ahmed*

Chemical Sciences Division, Lawrence Berkeley National Laboratory, Berkeley, California 94720

Received: March 8, 2008; Revised Manuscript Received: April 24, 2008

In this work, we report on the vacuum-ultraviolet (VUV) photoionization of small methanol and methanol–water clusters. Clusters of methanol with water are generated via co-expansion of the gas phase constituents in a continuous supersonic jet expansion of methanol and water seeded in Ar. The resulting clusters are investigated by single photon ionization with tunable vacuum-ultraviolet synchrotron radiation and mass analyzed using reflectron mass spectrometry. Protonated methanol clusters of the form $(\text{CH}_3\text{OH})_n\text{H}^+$ ($n = 1–12$) dominate the mass spectrum below the ionization energy of the methanol monomer. With an increase in water concentration, small amounts of mixed clusters of the form $(\text{CH}_3\text{OH})_m(\text{H}_2\text{O})_n\text{H}^+$ ($n = 2–11$) are detected. The only unprotonated species observed in this work are the methanol monomer and dimer. Appearance energies are obtained from the photoionization efficiency (PIE) curves for CH_3OH^+ , $(\text{CH}_3\text{OH})_2^+$, $(\text{CH}_3\text{OH})_n\text{H}^+$ ($n = 1–9$), and $(\text{CH}_3\text{OH})_m(\text{H}_2\text{O})_n\text{H}^+$ ($n = 2–9$) as a function of photon energy. With an increase in the water content in the molecular beam, there is an enhancement of photoionization intensity for the methanol dimer and protonated methanol monomer at threshold. These results are compared and contrasted to previous experimental observations.

Introduction

Photoionization studies of hydrogen bonded clusters provide insight into the thermodynamic and bonding properties of these systems. There have been numerous studies of methanol and methanol–water clusters utilizing a variety of ionization schemes.^{1–10} Initial work has focused on ion molecule reactions within these clusters upon photoionization. Recently, there has been a resurgence in the number of fundamental studies of hydrogen bonded clusters,¹¹ arising from the importance that these systems play in the astrochemical processing of hydrocarbons,¹² and local structure of mixed liquids.¹³ The photoionization properties of alcohol–water clusters is also important in the analytical chemistry community.¹⁴ Frequently, methanol is used as a dopant to facilitate ionization in atmospheric pressure photoionization. It is believed that the addition of methanol leads to cluster formation and a lowering of the ionization energy of the system.¹⁴

Recently, we have initiated a program to study the photoionization dynamics of hydrogen bonded systems upon vacuum-ultraviolet (VUV) irradiation. Measurements of photoionization onsets and mass spectra afford a window to deciphering fragmentation mechanisms and thermodynamic properties that have hitherto not been possible. While there has been a plethora of experimental work on methanol and mixed methanol–water clusters, there are certain outstanding questions remaining. The appearance of magic numbers, that is, cluster ions with enhanced intensities compared to neighboring masses, and the formation of mixed methanol–water cluster ions from pure methanol upon ionization have led to much debate in the literature.¹⁵ The fragmentation of these fragile hydrogen bonded clusters upon ionization has been studied in detail. However, the difference in proton transfer mechanisms of the two different hydrogens

in methanol, for example, the hydrogens bonded to the methyl group and to oxygen, remains ambiguous. This would make the ionization of methanol different from that of water, where there are two equivalent hydrogens. The changes in ionization properties upon clustering also allows for systematic trends to be studied utilizing tunable sources of ionization.

In a very early study, Kebarle and co-workers irradiated water–methanol vapor mixtures with a 100 keV proton beam in a high pressure mass spectrometer.² They observed series of clusters comprising $(\text{CH}_3\text{OH})_m(\text{H}_2\text{O})_n\text{H}^+$ where methanol is taken up preferentially in clusters of small size and water is taken up in the large ones ($m + n > 9$). They suggested that the proton is preferentially solvated by water in mixed water–methanol solutions. Stace and Shukla⁶ performed electron-impact ionization of mixed water–methanol clusters generated in an adiabatic expansion and observed a similar series of protonated clusters of the formula $(\text{CH}_3\text{OH})_m(\text{H}_2\text{O})_n\text{H}^+$ up to $m + n < 25$. Analysis of the metastable peak intensities showed that the proton is preferentially attached to methanol up to $n = 9$ and then it switches over to water. This result suggests that, upon ionization, neutral water elimination is the predominant loss channel for small cluster ions while larger cluster ions decompose by losing an alcohol. These results were explained by invoking the strength of ion–dipole interactions and the polarizability of the water–methanol clusters.

A very detailed study of mixed water–alcohol clusters to probe the structure and reactivity of these hydrogen bonded systems was performed by Garvey and co-workers.¹⁵ For methanol, they observed protonated methanol clusters complexed with one and two water molecules. They also observed enhanced stability (magic number) for $(\text{CH}_3\text{OH})_9(\text{H}_2\text{O})\text{H}^+$ and $(\text{CH}_3\text{OH})_{10}(\text{H}_2\text{O})_2\text{H}^+$. Similar behavior was observed for water clustered with ethanol, 1- and 2-propanol, as well as neat alcohol clusters. For pure alcohol, they concluded that the water component observed in the cluster ions of neat alcohol was produced by intracluster ion–molecule reactions. Castleman and

[†] Part of the “Stephen R. Leone Festschrift”.

* To whom correspondence should be addressed. Telephone: (510) 486-6355. Fax: (510) 486-5311. E-mail: MAhmed@lbl.gov.

co-workers⁴ observed similar behavior for $(\text{CH}_3\text{OH})_m(\text{H}_2\text{O})\text{H}^+$ ($m \geq 7$) upon multiphoton ionization of neat methanol clusters. Thermodynamic stability of intermediate cluster structures followed by proton transfer was suggested to give rise to the observed distribution. The similarity of observed cluster ion distributions formed from both neat alcohol and mixed methanol–water clusters suggests that it is the stability of the ion products that dictates the final cluster ion distribution rather than the initial composition of the neutral beam.¹⁵ In other words, in the case of methanol, ion–molecule reactions within the photoionized clusters lead to the formation of mixed clusters of the form $(\text{CH}_3\text{OH})_m(\text{H}_2\text{O})_n\text{H}^+$ from a neat methanol cluster beam.

Castleman and co-workers¹⁶ very early on also showed that mixed water–methanol cluster ions give rise to magic numbers for structures $(\text{CH}_3\text{OH})_m(\text{H}_2\text{O})_n\text{H}^+$ at $m + n = 21$, $0 \leq m \leq 8$ due to the enhanced stability of the dodecahedral cage structure in the mixed clusters. Fixed frequency VUV lasers at 10.5^{10,17} and 26.5 eV¹⁸ have been used to single photon ionize methanol cluster beams. Shi et al.¹⁰ claimed that the protonated trimer is the most intense peak (magic number), with protonated clusters being observed up to the pentamer. The authors attempted to correlate the measured ion distribution to the neutral cluster population. In contrast to the results at 10.5 eV, photoionization at 26.5 eV gives rise to the protonated dimer as the most dominant and protonated clusters $(\text{CH}_3\text{OH})_n\text{H}^+$ are detected up to $n = 10$. The authors argued that the depletion in the dimer signal in the 10.5 eV experiments is due to a near threshold ionization of the trimer at this wavelength leading to a reduced cross section for ionization. It is important to point out that these cross sections are unknown. In the same work, the authors state that the excess energy available is removed by the departing electron.

Nishi and Yamamoto⁷ created mixed clusters of a number of molecules with water by adiabatic expansion of liquid jets into vacuum. The resulting cluster beams were electron-impact ionized and quantitatively analyzed using mass spectrometry, which allowed for the determination of the stability of the hydrated clusters. They found that the cluster ions produced by this method provide a signature of the neutral cluster distribution and also to the structure of the original liquid solution itself. Following on from this work, Wakisaka et al.¹⁹ performed mass spectrometry of binary mixtures to explore nonideal mixing. They found that methanol added to water leads to a substitution mechanism; that is, water molecules are progressively replaced by methanol in the hydrogen bonded structures. Raina and Kulkarni¹³ also suggest that the ion cluster distribution of methanol–water mixtures provides information about the neutral binary vapor, which in turn reflects the structure of the liquid itself.

A major factor in utilizing soft ionization techniques that is provided by VUV light is to be able to decipher ionization mechanisms. The absence of unprotonated clusters in the mass spectrum upon photoionization is one of the most striking observations in the mass spectrometry of hydrogen bonded clusters. It is suggested that proton transfer reactions are very efficient within the ionized clusters and that the vertical ionization threshold leading to direct formation of unprotonated species is probably higher than the barrier to proton transfer. Systematic studies with tunable VUV light should shed light on these relative thresholds and fragmentation pathways. Early work by Cook et al.¹ utilized the University of Wisconsin synchrotron to photoionize an alcohol cluster beam. Appearance energies (shown in parentheses in eV) for CH_3OH^+ (10.84),

$(\text{CH}_3\text{OH})\text{H}^+$ (10.2), $(\text{CH}_3\text{OH})_2\text{H}^+$ (9.8), $(\text{CH}_3\text{OH})_3\text{H}^+$ (9.5), and $(\text{CH}_3\text{OH})_4\text{H}^+$ (9.3) were reported in that work. The authors did not observe any unprotonated clusters. From the dependence of cluster ion intensities on source conditions, estimates were provided for the heats of formation for methanol clusters.

Booze and Baer²⁰ utilizing coincidence techniques in conjunction with synchrotron radiation reported detecting $(\text{CH}_3\text{OH})_2^+$ at 10.2 eV photon energy. By comparing peak intensities and widths of the protonated dimer $(\text{CH}_3\text{OH})_2\text{H}^+$ with $(\text{CH}_3\text{OH})_2^+$, they concluded that dissociative photoionization gave rise to the protonated dimer. Tomoda and Kumara²¹ utilizing He I radiation reported the vertical ionization energy of the methanol dimer $((\text{CH}_3\text{OH})_2)$ to be 10.4 eV. Martrenchard-Barra et al.²² studied the proton transfer mechanism by performing threshold coincidence measurements with VUV radiation. They report a vertical ionization energy of 9.7 ± 0.05 eV for $(\text{CH}_3\text{OH})_2^+$ and the appearance energy for the protonated methanol ion $(\text{CH}_3\text{OH})\text{H}^+$ to be 10.15 ± 0.05 eV. By performing isotopic and threshold ionization studies, the authors surmised that two proton transfer mechanisms take place: one involves the methyl group which is exothermic but with a barrier, and the proton transfer from the hydroxyl group occurs at threshold without a barrier. Lee et al.²³ have performed extensive mass spectrometric and molecular orbital studies of electron impact ionized methanol clusters with particular emphasis on the methanol dimer. They proposed that ion-neutral complexes of the type $[\text{CH}_3\text{OH}_2^+ \cdots \text{O}(\text{H})\text{CH}_2]$ and $[\text{CH}_3\text{OH}_2^+ \cdots \text{OCH}_3]$ lead to the formation of the protonated species CH_3OH_2^+ with concomitant elimination of CH_2OH and OCH_3 , respectively. However, the calculated barriers and thresholds do not agree qualitatively with the results of Martrenchard-Barra et al.²² Tsai et al.²⁴ photoionized the methanol dimer using a tunable VUV laser in conjunction with deuteration studies and also performed extensive *ab initio* calculations to get a handle on the mechanism of proton transfer in this system. In the range of 10.49–10.9 eV, the probability of the proton transfer from the hydroxyl group increased with photon energy. Using *ab initio* methods, the authors found four stable structures of the methanol dimer; one of these $[\text{CD}_3\text{OHD}^+ \cdots \text{CD}_2\text{OH}]$ is supposed to play a major role in the deuteron transfer reaction. The reported energy barriers and pathways to proton and deuteron transfer from the methanol dimer is at variance from those calculated earlier by Lee et al.²³

We have performed a systematic study utilizing tunable VUV irradiation in conjunction with reflectron mass spectrometry to shed light on some of the outstanding questions that remain on the photoionization mechanism of hydrogen bonded clusters of methanol and methanol with water. The variation in the intensities of mass spectral peaks with the addition of water to methanol at various photon energies is discussed and contrasted with previous work. We will show that photoionization mass spectrometry under our clustering conditions does not reflect the composition of the original liquid solution. Appearance energies for a number of protonated methanol and methanol–water clusters are reported for the first time.

Experimental Section

The experiments are performed in a chamber incorporating a continuous supersonic expansion of methanol and methanol–water mixtures to produce clusters. The apparatus is coupled to a three meter vacuum ultraviolet monochromator on the Chemical Dynamics Beamline (9.0.2) located at the Advanced Light Source. This apparatus is recently discussed for generating pure water clusters,²⁵ and relatively minor changes are intro-

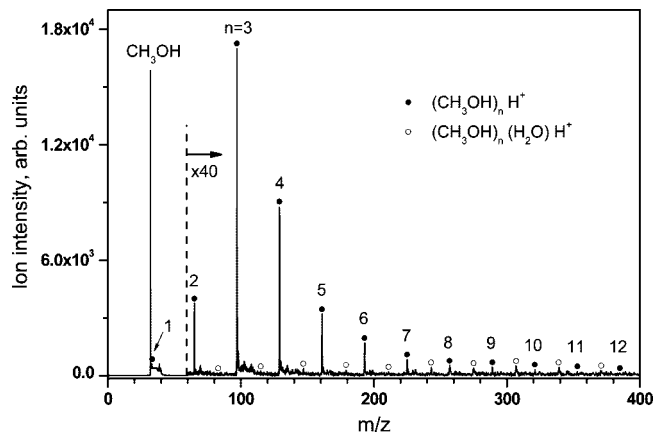


Figure 1. Time-of-flight mass spectrum of 5:1 methanol–water solution corresponding to a methanol vapor mole fraction of 0.90. Ionization is performed with 11 eV light. Starting from $m/z = 60$, the ion intensity is increased by a factor of 40. Filled circles (\bullet) indicate peaks associated with protonated methanol cluster cations ($(\text{CH}_3\text{OH})_n\text{H}^+$), and open circles (\circ) denote protonated methanol–single water cluster cations ($(\text{CH}_3\text{OH})_n(\text{H}_2\text{O})\text{H}^+$). Additionally, a peak corresponding to unprotonated methanol monomer ($m/z = 32$) is shown.

duced, such as to produce a continuous supersonic molecular beam of mixed methanol–water clusters. Neutral clusters are formed in a supersonic expansion of 114 kPa of Ar with seeded methanol and methanol–water vapor through a 100 μm nozzle orifice and pass through a 1 mm conical skimmer located 20 mm downstream. Ar is passed through a bubbler containing either pure methanol liquid or methanol–water mixtures. Methanol with purity higher than 99.8% and deionized water are used for preparation of samples. The pressures in the source and main chambers are 4.2×10^{-2} and 2.4×10^{-4} Pa, respectively, under normal operating conditions.

In the main chamber, the neutral cluster beam is interrogated in the ionization region of a commercial reflectron time-of-flight (TOF) mass spectrometer by tunable VUV radiation. Since the synchrotron light is quasi-continuous (500 MHz), a start pulse for the TOF ion packet is provided by pulsing the ion optics electric potential. The accelerator and repeller plates of the ion optics are biased at the same potential (1600 V), and ions are extracted by fast switching of the repeller plate to 1900 V with a pulse width of 2.5 μs . Ions are accelerated perpendicularly to their initial velocity direction through the field free region towards the reflectron. Ions, reflected in the electrostatic field of the ion mirror, are detected by a microchannel plate (MCP) installed at the end of the second field free region. The time-dependent electrical signal from the MCP is amplified by a fast preamplifier, collected by a multichannel-scalar card and thereafter integrated with a PC computer. Time-of-flight spectra are recorded for the photon energy range between 9 and 15 eV. The typical photon energy step size used for these experiments is 50 meV, and the accumulation time at each photon energy is 300 s. The photoionization efficiency curves of the clusters are obtained by integrating over the peaks in the mass spectrum at each photon energy and normalized by the photon flux. The synchrotron VUV photon flux is measured by a Si photodiode. Argon absorption lines are used for energy calibration of the PIE spectra.

Results and Discussion

Mass Spectrometry of Methanol Clusters. Mass spectra of neat methanol and methanol–water mixtures were collected between photon energies of 9 and 15 eV. Figure 1 shows a

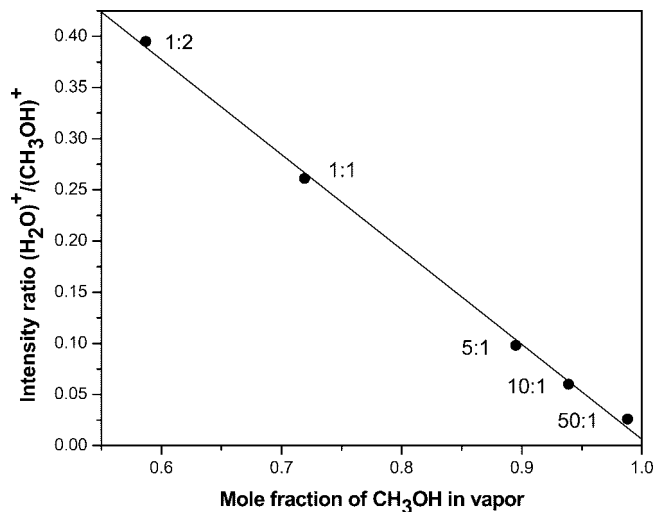


Figure 2. Intensity of H_2O ($m/z = 18$) normalized to intensity of methanol peak ($m/z = 32$) at 13 eV for various methanol–water concentrations. The ratio of methanol to water solution by volume is indicated next to each symbol. The solid line represents a linear fit to the experimental data.

mass spectrum of a supersonic expansion of the vapor above a 5:1 by volume methanol–water solution recorded with a photon energy of 11 eV. The methanol monomer (IE = 10.8 eV) dominates the mass spectrum followed by protonated methanol clusters ($(\text{CH}_3\text{OH})_n\text{H}^+$). In addition, a weak series composed of $(\text{CH}_3\text{OH})_n(\text{H}_2\text{O})\text{H}^+$ is also observed. A peak at $m/z = 64$ (not shown in the figure) is assigned to the methanol dimer $(\text{CH}_3\text{OH})_2^+$, with this being the only unprotonated cluster apart from parent methanol and water being detected. The absence of unprotonated cluster peaks arises from the instability of the ionized clusters and efficient proton transfer that occurs upon photoionization even at threshold energies.

There have been reports in the literature^{13,26} that molecular beam mass spectrometry allows for determination of the bonding properties of mixtures. In other words, the local structure of mixed liquid systems is retained in memory upon being ionized in a molecular beam. These experiments are different from the adiabatic expansion of liquid jets as has been practiced by Nishi and Yamamoto⁷ where it is possible to sample directly from the liquid. We used tabulated values²⁷ of vapor phase constituents of methanol–water solutions to calculate the mole fraction of methanol vapor in the reservoir containing the solution. The methanol–water volume mixing ratios of 50:1, 10:1, 5:1, 1:1, and 1:2 in solution correspond to methanol vapor mole fractions of 0.99, 0.94, 0.90, 0.72, and 0.59, respectively. These values correlate in a linear manner with the detected water/methanol monomer ratio shown in Figure 2. This plot provides evidence that in our experiments we are entraining the vapor component of the mixture in the carrier gas and subsequent cluster formation takes place upon supersonic expansion from the nozzle. This would suggest that in our experimental configuration we are only sensitive to the vapor component above the liquid solution. The fact that we observe clusters in our supersonic expansion suggests significant cooling is being provided in the molecular beam.

The peak intensities of protonated methanol and methanol–water clusters recorded under methanol vapor mole fractions of 0.99, 0.94, 0.90, 0.72, and 0.59 at photon energies of 10 and 12 eV are shown in Figure 3. The cluster ion distributions have been normalized to the protonated methanol monomer intensity recorded at 12 eV to allow for a comparison of systematic trends upon increased water concentration in the solution.

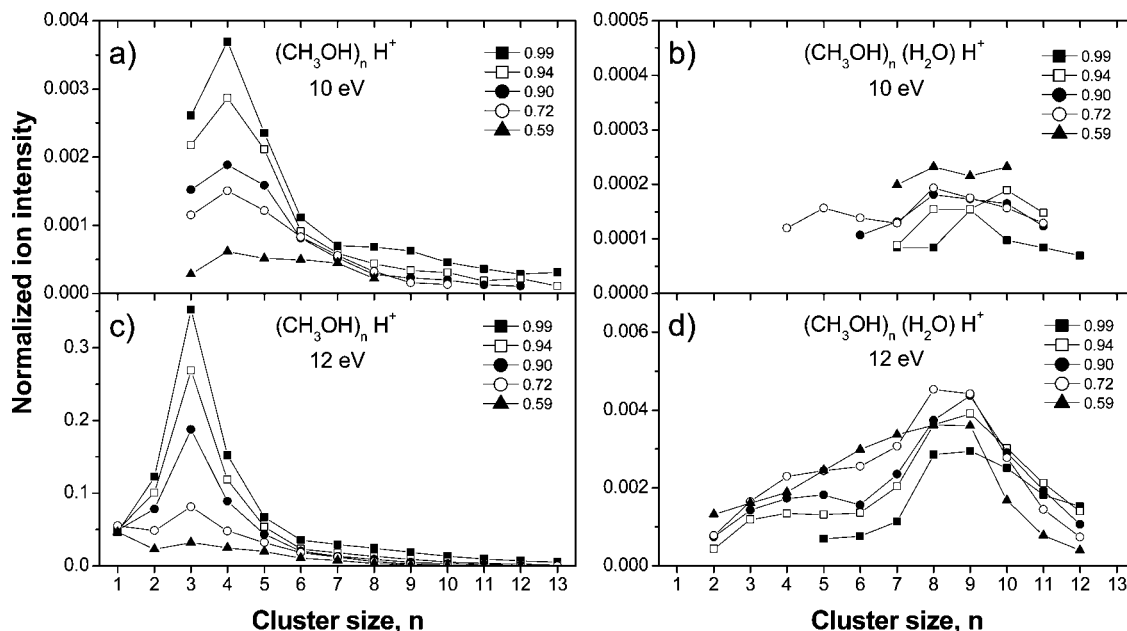


Figure 3. Ion intensities of protonated methanol and methanol–water clusters at various photon energies and methanol–water mixtures. Signals have been normalized to the intensity of $(\text{CH}_3\text{OH})_4^+\text{H}^+$ at 10 eV. The mole fraction of methanol in vapor above the methanol–water solution is shown in the inset of each panel. (a) $(\text{CH}_3\text{OH})_n\text{H}^+$ at 10.0 eV; (b) $(\text{CH}_3\text{OH})_n(\text{H}_2\text{O})\text{H}^+$ at 10.0 eV; (c) $(\text{CH}_3\text{OH})_n\text{H}^+$ at 12.0 eV; and (d) $(\text{CH}_3\text{OH})_n(\text{H}_2\text{O})\text{H}^+$ at 12.0 eV.

In the protonated methanol cluster series recorded at 10 eV (Figure 3a), $(\text{CH}_3\text{OH})_4\text{H}^+$ is the most abundant peak, and then there is a rapid drop-off in the signal down to cluster sizes $n = 13$. In the protonated methanol–single water cluster series $((\text{CH}_3\text{OH})_n(\text{H}_2\text{O})\text{H}^+)$, only cluster sizes $n = 4–12$ are seen with any intensity (Figure 3b). An increase of the photon energy to 12 eV shifts the intensity of the protonated clusters to $(\text{CH}_3\text{OH})_3\text{H}^+$ and is followed then by a smooth decrease in intensity up to $n = 13$ (shown in Figure 3c). There is a much larger change in the methanol–single water cluster series $((\text{CH}_3\text{OH})_n(\text{H}_2\text{O})\text{H}^+)$ upon increasing the photon energy (Figure 3d). There is enhanced intensity for clusters $n = 8$ and 9, and mixed water clusters are seen between $n = 2$ and 12. The nature of these enhancements and their dependence on water concentration will be discussed below.

The appearance of protonated methanol upon ionization has been observed previously in a number of studies involving electron impact,⁵ multiphoton^{3,4,28} and single photon ionization.^{10,17,18} It is believed that the ionization of the neutral hydrogen bonded clusters leads to the formation of the protonated cluster ions via rapid proton transfer and fragmentation. The distribution of protonated cluster ions seen in this work (Figure 3c) is very similar to that observed utilizing multiphoton⁴ ionization and 10.5¹⁷ and 26.5¹⁸ eV single photon ionization. Previous photoionization studies at 10.5 eV show that the protonated trimer is stronger in intensity compared to the dimer.^{10,17} It was speculated that the change in ion intensities between the dimer and trimer arose either due to different photoionization cross sections¹⁸ for these species or because there is a magic number enhancement in the tetramer neutral precursor¹⁰ appearing in the mass spectrum as the protonated trimer. In this work, we used tunable VUV to measure photoionization efficiency curves for $(\text{CH}_3\text{OH})_2\text{H}^+$ and $(\text{CH}_3\text{OH})_3\text{H}^+$, and these are plotted for the photon energy range of 9–14.6 eV for a pure methanol cluster beam (Figure 4). At 10.5 eV, the ratio of protonated trimer to dimer intensity is about 7.3, and at around 14 eV the curves cross over. This switching over of photoionization curves could explain the difference in results between the 10.5 eV

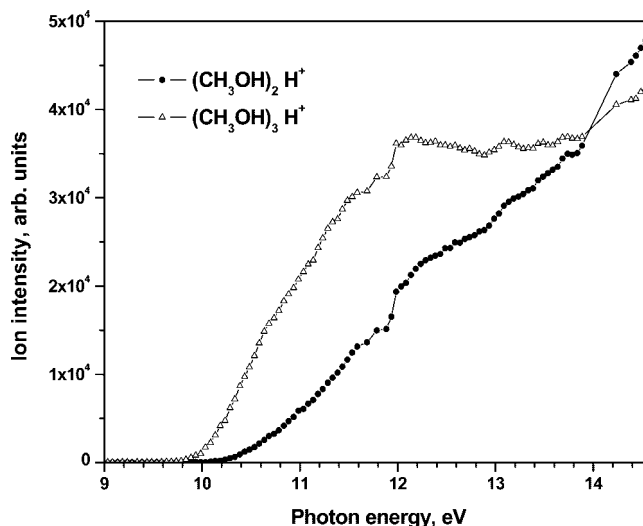


Figure 4. Photoionization efficiency curves for protonated methanol dimer ($m/z = 65$) and trimer ($m/z = 97$).

work^{9,10} and results seen with higher photon energies¹⁸ where the protonated dimer is more abundant than the trimer. This, however, does not resolve the question of whether the observed ion distributions arise from magic number distributions or from an enhanced photoionization cross section for the protonated trimer at lower photon energies. It is apparent that attempting to determine magic numbers solely from data collected at a single photon energy as attempted in earlier work does not reflect the complexity of how the photoionization cross section, fragmentation dynamics, and populations change over an energy range.

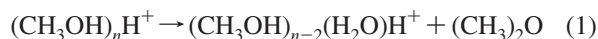
Mass Spectrometry of Mixed Methanol–Water Clusters. In addition to the main protonated methanol series of clusters, a second much weaker series of methanol–water clusters with the formula $(\text{CH}_3\text{OH})_n(\text{H}_2\text{O})\text{H}^+$ are observed in Figure 1. Interestingly, Bernstein and co-workers did not observe this series with either 10.5¹⁷ or 26.5¹⁸ eV single photon ionization.

TABLE 1: Appearance Energies for Pure and Protonated Methanol and Methanol–Water Clusters Evaluated from Photoionization Efficiency Curves

ion	appearance energy, eV (this work)	literature values, eV
CH_3OH^+	10.80 ± 0.05	$10.84,$ ^a 10.84 ± 0.01 ^b
$(\text{CH}_3\text{OH})_2^+$	9.8 ± 0.2	$9.8,$ ^c 9.7 ± 0.05 ^d
$(\text{CH}_3\text{OH})\text{H}^+$	10.2 ± 0.1	$10.2,$ ^a 10.15 ± 0.05 ^d
$(\text{CH}_3\text{OH})_2\text{H}^+$	10.1 ± 0.1	9.8 ^a
$(\text{CH}_3\text{OH})_3\text{H}^+$	9.8 ± 0.1	9.5 ^a
$(\text{CH}_3\text{OH})_4\text{H}^+$	9.8 ± 0.1	9.3 ^a
$(\text{CH}_3\text{OH})_5\text{H}^+$	9.6 ± 0.1	
$(\text{CH}_3\text{OH})_6\text{H}^+$	9.6 ± 0.1	
$(\text{CH}_3\text{OH})_7\text{H}^+$	9.8 ± 0.1	
$(\text{CH}_3\text{OH})_8\text{H}^+$	9.7 ± 0.1	
$(\text{CH}_3\text{OH})_9\text{H}^+$	9.8 ± 0.1	
$(\text{CH}_3\text{OH})_2(\text{H}_2\text{O})\text{H}^+$	10.1 ± 0.2	
$(\text{CH}_3\text{OH})_3(\text{H}_2\text{O})\text{H}^+$	10.2 ± 0.1	
$(\text{CH}_3\text{OH})_4(\text{H}_2\text{O})\text{H}^+$	9.8 ± 0.1	
$(\text{CH}_3\text{OH})_5(\text{H}_2\text{O})\text{H}^+$	9.9 ± 0.1	
$(\text{CH}_3\text{OH})_6(\text{H}_2\text{O})\text{H}^+$	9.9 ± 0.1	
$(\text{CH}_3\text{OH})_7(\text{H}_2\text{O})\text{H}^+$	9.8 ± 0.1	
$(\text{CH}_3\text{OH})_8(\text{H}_2\text{O})\text{H}^+$	9.7 ± 0.1	
$(\text{CH}_3\text{OH})_9(\text{H}_2\text{O})\text{H}^+$	9.6 ± 0.1	

^a Reference 1. ^b Reference 33. ^c Reference 21. ^d Reference 22.

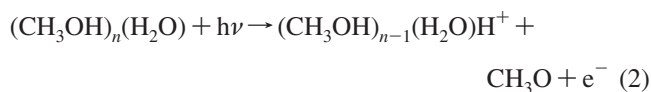
In our work, these clusters can be observed around 9.8 eV (appearance energies are reported in Table 1) and the intensities increase with photon energy (Figure 3b and d). There is enhanced intensity for clusters $n = 8$ and 9 in this series. This kind of behavior has been observed earlier in electron impact ionization of methanol and methanol–water clusters by Garvey et al.¹⁵ and Elshall et al.²⁹ The enhanced intensity of $(\text{CH}_3\text{OH})_9(\text{H}_2\text{O})\text{H}^+$ was attributed to complete solvation of a core H_3O^+ ion by nine methanol molecules surrounding it and leading to the maximum number of hydrogen bonds.³⁰ The authors also suggested that an efficient proton transfer takes place from methanol to be incorporated into a fully solvated hydronium ion. Castleman and co-workers also observed the formation of mixed methanol–water clusters upon ionization of pure alcohol clusters using multiphoton ionization.^{3,4,28} Using reflectron mass spectrometry and collision studies of ion–molecule cluster reactions in a flow cell, they suggested that it is the elimination of dimethyl ether ($(\text{CH}_3)_2\text{O}$) from protonated methanol clusters that leads to the mixed cluster formation:



It was also suggested that this reaction occurs for size $n \geq 9$, since the smallest cluster observed in the works of Garvey et al.¹⁵ and Castleman and co-workers^{3,4,28} is $(\text{CH}_3\text{OH})_7(\text{H}_2\text{O})\text{H}^+$. Morgan and Castleman²⁸ suggest that this reaction does not occur for the smaller clusters, since the formation of a methyl bound complex intermediate is not facile. Garvey and co-workers¹⁵ comment that the distributions of the mixed cluster ions arising from either neat alcohol or alcohol–water mixtures are quite similar, but they do not show any experimental data that can be compared with our results. With the addition of more water in the mixture, we observe an enhancement of the signal toward smaller clusters ($n = 2–7$) (Figure 3d); however, under our experimental conditions, it is the 8- and 9-mer which dominates the mixed cluster series. At each photon energy used, the intensity of all mixed clusters increases with the addition of water, as shown in Figure 3b and d.

The mixed cluster series could originate from two sources: from fragmentation of pure methanol clusters, as originally

suggested by Castleman and co-workers^{3,4} and shown in eq 1, and also from photoionization of a mixed methanol–water cluster, as shown in eq 2



The appearance of the mixed cluster ions in the pure methanol expansion probably arises from the first scheme (eq 1), and with the addition of water, the second scheme (eq 2) will play an increased role in the ion distributions. The appearance of the smaller mixed clusters ($n = 2–6$) with increased photon energy (compare Figure 3b and d) could arise from the ionization energy being higher for the smaller clusters. They could also arise from fragmentation of larger clusters upon increased photon energy. However, since the relative cluster ion distributions remain the same between 12 and 14 eV (not shown), this mechanism can be safely discounted in this energy range.

Photoionization Efficiency Curves of Methanol and Methanol–Water Clusters. A primary motivation of probing the photoionization dynamics of mixed methanol–water clusters with variable photon energy is to observe a shift in ionization when water becomes available for ionization at 12.6 eV. There is no dramatic shift in the intensities of peaks in the mass spectra with a change in photon energy above 12.6 eV apart from the detection of the water monomer. No pure water clusters are observed under our expansion conditions. Previous work from our group²⁵ has shown that the ionization energy of water decreases upon clustering, reaching an asymptotic limit of around 10.6 eV for clusters of size $n > 20$. A similar analysis was performed on the mixed methanol–water clusters in this work. PIE curves were recorded for detectable masses in the range of 9–15 eV for various methanol–water solutions. The PIE curves for a methanol vapor mole fraction of 0.72 are shown in Figure 5 for the photon energy range of 9–11 eV. The left column of Figure 5 shows the PIE curves for protonated methanol monomer and methanol clusters ($(\text{CH}_3\text{OH})_n\text{H}^+$) for $n = 2–6$, and the right column shows curves for methanol (CH_3OH^+) and protonated methanol–water ($(\text{CH}_3\text{OH})_n(\text{H}_2\text{O})\text{H}^+$) clusters for $n = 2–6$. The corresponding appearance energies are reported in Table 1. All of the appearance energies of protonated methanol clusters for $n \geq 3$ and protonated methanol with water monomer clusters for $n \geq 4$ are in the range of 9.6–9.9 eV. The values of the appearance energy obtained in this work disagree with that of Cook et al.¹ for clusters larger than the protonated monomer which are also shown in Table 1 for comparison.

The appearance energy values obtained for unprotonated methanol monomer, dimer, and protonated monomer are 10.80 ± 0.05 , 9.8 ± 0.2 , and 10.2 ± 0.1 , respectively. Cook et al.¹ observed a PIE curve for $m/z = 33$ (protonated monomer) with an appearance energy of 10.2 eV which correlates well to the value obtained in this work. They observed a similar shoulder between this appearance energy and the sudden rise around 10.8 eV. Cook et al.¹ operated a continuous molecular beam of pure methanol with pressure between 13.3 and 26.7 kPa. In this work, a seeded expansion of methanol–water vapor in Ar is used and the shoulder only becomes pronounced upon dilution of methanol with water. This suggests that addition of water perturbs the PIE curve in the threshold ionization region. In a coincidence study employing synchrotron radiation,²² the appearance energy of protonated methanol is reported to be 10.15 ± 0.05 eV and the unprotonated dimer is observed at 9.7 ± 0.05 eV, which agrees well within reported errors with our

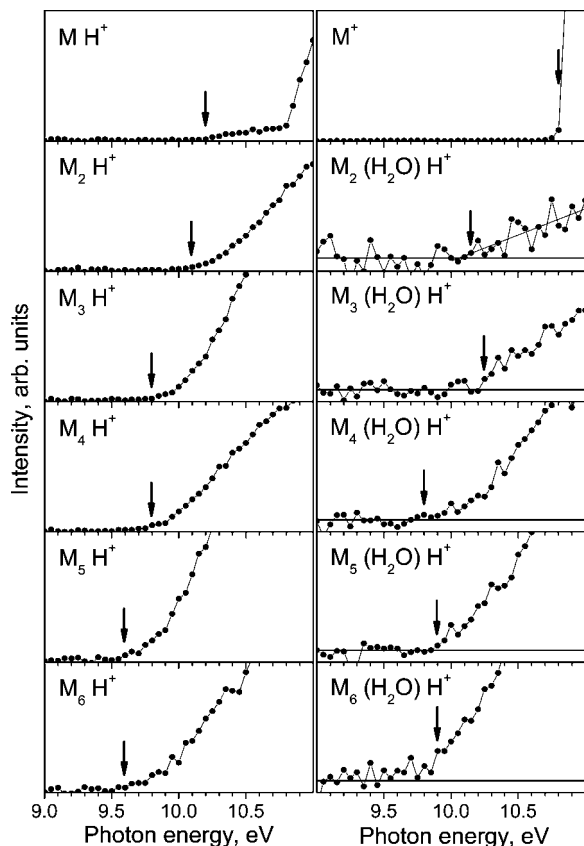


Figure 5. PIE curves for various species formed in an expansion of 0.72 mole fraction of methanol in vapor above the methanol–water solution. M denotes methanol (CH_3OH). PIE curves for protonated methanol monomer and methanol clusters ($(\text{CH}_3\text{OH})_n\text{H}^+$) for size $n = 2-6$ are shown in the left column; PIE curves for methanol cation (CH_3OH^+) and methanol–water clusters ($(\text{CH}_3\text{OH})_n(\text{H}_2\text{O})\text{H}^+$) for $n = 2-6$ are shown in the right column. Arrows show appearance energies. Additionally, for $(\text{CH}_3\text{OH})_2(\text{H}_2\text{O})\text{H}^+$, a line representing linear fit to the experimental data is shown.

values of 10.2 ± 0.1 and 9.8 ± 0.2 eV, respectively. Tsai et al.²⁴ and Lee et al.²³ performed *ab initio* calculations for the methanol dimer and reported vertical ionization energies of 9.74 and 10.18 eV, respectively. Tomoda and Kimura²¹ measured the photoelectron spectrum of the methanol dimer using a stripping technique. Analysis of their spectrum shows an onset at 9.8 eV followed by a sharp rise in intensity at 10.7 eV peaking at 11.21 eV. Tsai et al.²⁴ photoionized the CD_3OH dimer utilizing tunable VUV radiation between 10.49 and 10.91 eV and probed the reaction products by TOF mass spectrometry. A plot of the ratio of $(\text{CD}_3\text{OH})\text{H}^+ / (\text{CD}_3\text{OH})\text{D}^+$ versus photon energy shows a dramatic enhancement of signal around 10.8 eV. This was rationalized by the authors²⁴ to mean that the rate of proton transfer from the hydroxyl part of the photoionized dimer $(\text{CD}_3\text{OH})_2^+$ increases around this energy. We see a similar enhancement in signal in $(\text{CH}_3\text{OH})\text{H}^+$ around 10.8 eV. This could arise from either better Franck–Condon factors between the neutral and ionized species or enhanced proton transfer rates as was suggested by Tsai et al.²⁴ It appears that proton transfer might be giving rise to this enhancement as opposed to photoionization dynamics, since this effect is pronounced with the addition of more water to the solution.

Threshold Effects on PIEs upon Addition of Water. PIE curves similar to those shown in Figure 5 were recorded for methanol vapor mole fractions of 0.99, 0.94, 0.90, and 0.59, and they are not shown here for brevity. The shapes of these curves did not change with the mixing ratio apart for two peaks

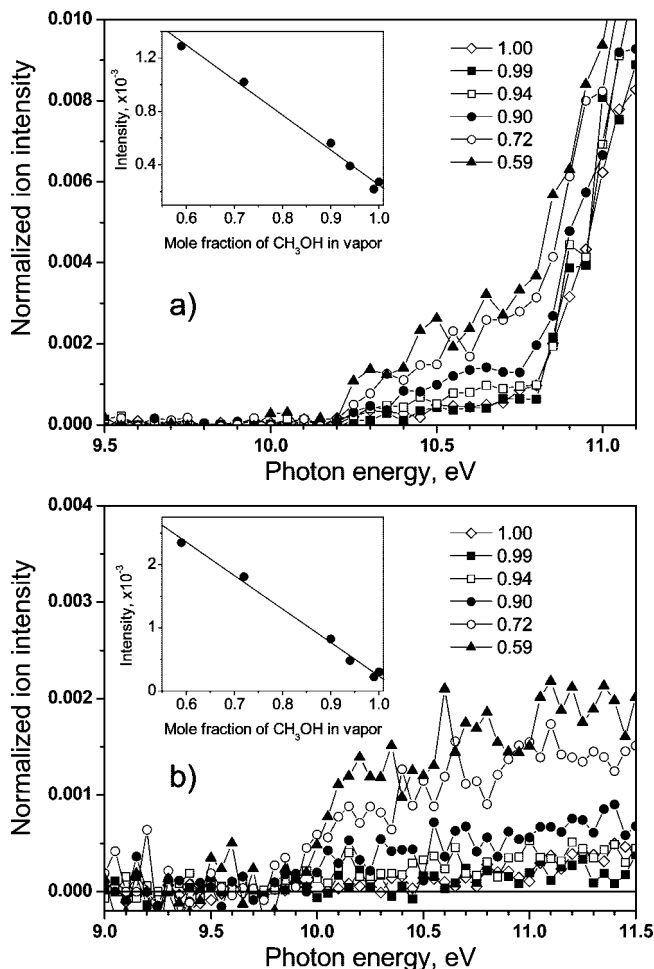
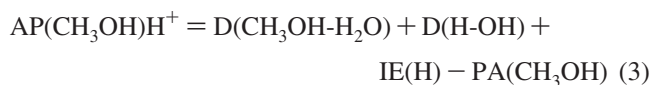


Figure 6. PIE curves for (a) protonated methanol ($m/z = 33$) and (b) unprotonated methanol dimer ($m/z = 64$) at various methanol–water concentrations. Mole fractions of methanol in vapor above methanol–water solution are shown in labels. The dependencies of area of PIE peaks (a) from 10.0 to 10.8 eV and (b) from 9.7 to 11.5 eV on the mole fraction of methanol in vapor are shown in the insets together with a linear fit.

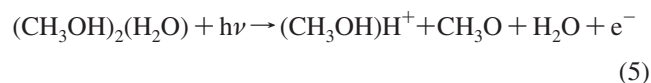
associated with protonated methanol monomer $(\text{CH}_3\text{OH})\text{H}^+$ and unprotonated methanol dimer $(\text{CH}_3\text{OH})_2^+$, and these are shown in Figure 6. The curves have been normalized to the signal of methanol monomer at 13 eV. For protonated methanol, the appearance energy is 10.2 eV, beyond which there is a gentle rise in intensity up to 10.8 eV following which there is a rapid rise. With an increase in water content in the mixture, the portion of the spectrum between 10.2 and 10.8 eV rises up, creating a shoulder between these two energies. Integrating the area in this shoulder between onset and 10.8 eV and plotting it against the mole fraction of methanol in vapor above the methanol–water mixture yields an inverse linear correlation which is plotted in the inset of Figure 6a. For $(\text{CH}_3\text{OH})_2^+$, the PIE curves shown in Figure 6b, also display a similar trend. The PIE curves rise very gently from an onset of 9.8 eV. With an increase in water contribution to the solution, the onset remains the same, but the shape changes with the slope, becoming almost a plateau after the initial rise. To quantify the change in shape of the PIE curve, the area between 9.7 and 11.5 eV is plotted in the inset with the change in methanol concentration in vapor. The linear relationships seen in the insets of Figure 6 suggest that water is contributing in a similar way to the formation of the protonated monomer and the unprotonated dimer.

With the addition of water, it is probable that in addition to the methanol dimer $(\text{CH}_3\text{OH})_2$ there will also be mixed clusters of the form $(\text{CH}_3\text{OH})_n(\text{H}_2\text{O})_m$ present in the molecular beam. Ionization and proton transfer from this species could also give rise to protonated methanol which could give rise to the increase in signal between threshold and 10.8 eV seen with increase in water concentration in the molecular beam. However, a thermodynamic analysis involving the following cycle for a methanol–water dimer



where $\text{D}(\text{CH}_3\text{OH}-\text{H}_2\text{O})^{31} = 0.22$ eV; $\text{D}(\text{H}-\text{OH})^{32} = 5.1$ eV; $\text{IE}(\text{H})^{33} = 13.598$ eV; and $\text{PA}(\text{CH}_3\text{OH})^{33} = 7.82$ eV (D = dissociation energy; IE = ionization energy; and PA = proton affinity), suggests that the appearance energy of protonated methanol from a $(\text{CH}_3\text{OH})(\text{H}_2\text{O})$ dimer requires at least 11.1 eV for the reaction to proceed. We cannot evaluate proton transfer from methanol to water in this scheme, since that would give rise to CH_3OH^+ and the thermodynamic cycle would not be complete. However, a similar analysis for $(\text{CH}_3\text{OH})_2$ with $\text{D}(\text{CH}_3\text{OH}-\text{CH}_3\text{OH})^1 = 0.2$ eV; $\text{D}(\text{H}-\text{OCH}_3)^{24} = 4.51$ eV; $\text{D}(\text{H}-\text{CH}_2\text{OH})^{24} = 4.08$ eV; $\text{IE}(\text{H})^{33} = 13.598$ eV; and $\text{PA}(\text{CH}_3\text{OH})^{33} = 7.82$ eV predicts appearance energies of 10.06 and 10.49 eV for proton transfer from the methyl and hydroxyl group, respectively. Tsai et al.³⁴ using *ab initio* methods have calculated the various dissociation pathways possible upon ionization of a neutral methanol dimer $(\text{CD}_3\text{OH})_2$. According to their calculations performed at the B3LYP level with zero-point vibrational energy corrections, to form $\text{CD}_3\text{O} + \text{CD}_3\text{OH}_2^+$ and $\text{CD}_2\text{OH} + \text{CD}_3\text{OHD}^+$ requires 10.37 and 10.08 eV, respectively. Comparing these predicted appearance energies to our results would suggest that at threshold the ionized dimer fragments to $(\text{CH}_3\text{OH})\text{H}^+ + \text{CH}_3\text{O}$ and with increasing photon energy the second channel leading to $(\text{CH}_3\text{OH})\text{H}^+ + \text{CH}_2\text{OH}$ comes into play. While this analysis provides a reasonable explanation for the shape of the protonated monomer PIE, it still does not explain the increase in intensity at threshold upon addition of water.

It is possible that $(\text{CH}_3\text{OH})_2(\text{H}_2\text{O})$ could give rise to the observed trends upon photoionization.



To the best of our knowledge, there are no experimental measurements of the dissociation energy of a water monomer from a methanol dimer in the neutral state to guide us in formulating a thermodynamic cycle as was done for methanol dimer and the methanol–water dimer in the previous paragraph. However, using the appearance energies observed in this work, we can calculate an approximate strength of the dissociation energy, for separating H_2O and $(\text{CH}_3\text{OH})_2$. The appearance energy (ionization energy) for $(\text{CH}_3\text{OH})_2^+$ is 9.8 eV; the water contribution to the signal starts at 10 eV photon energy (Figure 6b). This would suggest that the bond dissociation energy is at least 0.2 eV. In the previous paragraph, we predict an appearance energy of 10.06 eV for $(\text{CH}_3\text{OH})\text{H}^+$ formation from the methanol dimer $(\text{CH}_3\text{OH})_2$. For eq 5, the bond dissociation energy between water and the methanol dimer will be the difference in the appearance energies of $(\text{CH}_3\text{OH})\text{H}^+$ and the water-dependent ion signal contribution which shows up at 10.2

eV in Figure 6a. This would suggest a bond dissociation energy of at least 0.14 eV in eq 5. While the derivations are necessarily crude, the energies are typical of the strength of hydrogen bonds calculated in water–methanol cluster systems.^{35–38}

With the addition of water in the solution, it is plausible that a water monomer will bind with a methanol dimer; the driving force would be the enhanced stability of a cyclic trimer where three hydrogen bonds can form. Masella and Flament³⁵ discuss the stability of these trimer species using *ab initio* calculations. They find that while $(\text{CH}_3\text{OH})_3$ is the most stable species, the $(\text{CH}_3\text{OH})_2(\text{H}_2\text{O})$ cluster is more stable than either $(\text{CH}_3\text{OH})(\text{H}_2\text{O})_2$ or $(\text{H}_2\text{O})_3$. It is also suggested that cooperative effects strongly stabilize the cyclic trimers when compared to the isolated dimers. Using a localized orbital theory approach, hydrogen bonds are the result of charge transfer from a lone pair of the donor (sp^3 orbital) to an antibonding σ^* orbital of the acceptor and this is reinforced in a cyclic cluster. Very recently, Mejia et al.³⁷ performed a theoretical study to map out the potential energy surfaces of a number of alcohol–water trimers, among which $(\text{CH}_3\text{OH})_2(\text{H}_2\text{O})$ was also studied. They suggested that structures with a cyclic pattern in which all the three hydrogen bonds are in O–H–O configuration and simultaneously act as proton donors–acceptors are much more stable when compared to structures with just two primary hydrogen bonds. It is plausible that this strength in hydrogen bonding and increase in binding energies will increase the population of the methanol–water trimer with addition of water to the system. It is also important to point out that this is a fairly minor channel which could give rise to intensity at $m/z = 33$ and 64 at threshold. The bulk of the signal in the PIE curves for $m/z = 33$ and 64 will arise from photoionization of the neutral dimer $(\text{CH}_3\text{OH})_2$. We had remarked earlier that Cook et al.¹ observed a shoulder in the PIE at threshold for the protonated monomer followed by a sharp rise at 10.8 eV. Our results show that this shoulder depends very strongly on the water content of the molecular beam and might suggest that the shape of the PIE curve observed in the work of Cook et al.¹ could be explained by water being present in their methanol molecular beam.

The decrease in the ionization energy between CH_3OH and $(\text{CH}_3\text{OH})_2$ is a general trend which is observed in hydrogen bonded systems (e.g., water, ammonia). Hydrogen bonding will cause a large destabilization of the highest occupied molecular orbital localized on the proton donor side. An examination of Table 1 shows that the most prominent change in ionization energy occurs when one moves from the monomer to the dimer. As remarked earlier, there are extreme geometry changes between the neutral and ionized clusters of methanol, which lead to subsequent proton transfer and fragmentation of the cluster. In our work with water clusters,²⁵ we observed similar fragmentation and OH elimination from the cluster. By carefully measuring these fragmentation properties using reflectron mass spectrometry, we were able to correlate the appearance energies to ionization energies of the neutral cluster. However, in this work, the fragmentation properties could not be studied in detail, since metastable peak signals were really low. Furthermore, the difference in proton transfer mechanisms of the two different hydrogens in methanol, for example, the hydrogens bonded to the methyl group and to oxygen, makes the ionization of methanol different from that of water, where there are two equivalent hydrogens. Hence, we cannot derive ionization energies of the neutral precursors of the corresponding parent. However, qualitatively, it is apparent that the appearance energies of the higher clusters do not change dramatically

beyond the protonated dimer, suggesting that added methanol or water does not affect the ionization dynamics profoundly.

Conclusion

In this work, we report on the study of VUV photoionization of small methanol and methanol–water clusters. Protonated methanol clusters of the form $(\text{CH}_3\text{OH})_n\text{H}^+$ ($n = 1-12$) dominate the mass spectrum below the ionization threshold of the methanol monomer. With an increase in water concentration, small amounts of mixed clusters of the form $(\text{CH}_3\text{OH})_n(\text{H}_2\text{O})\text{H}^+$ ($n = 2-11$) are detected. There is also some contribution to the mixed cluster signal from ion–molecule reactions within ionized pure methanol clusters. The only unprotonated species observed in this work are the methanol monomer and dimer. Appearance energies are obtained by evaluating photoionization efficiency curves for CH_3OH^+ , $(\text{CH}_3\text{OH})_2^+$, $(\text{CH}_3\text{OH})_n\text{H}^+$ ($n = 1-9$), and $(\text{CH}_3\text{OH})_n(\text{H}_2\text{O})\text{H}^+$ ($n = 2-9$) as a function of photon energy. The appearance energies of 10.2 ± 0.1 and 9.8 ± 0.2 eV for $(\text{CH}_3\text{OH})\text{H}^+$ and $(\text{CH}_3\text{OH})_2^+$, respectively, agree very well with literature values. With an increase in the water content in the molecular beam, there is substantial enhancement of photoionization intensity for protonated methanol monomer and unprotonated methanol dimer at threshold. This may be explained by enhanced formation of a cyclic trimer containing two methanol molecules and a water monomer connected via three hydrogen bonds.

Acknowledgment. This work was supported by the Director, Office of Energy Research, Office of Basic Energy Sciences, Chemical Sciences Division of the U.S. Department of Energy under Contract No. DE-AC02-05CH11231.

References and Notes

- (1) Cook, K. D.; Jones, G. G.; Taylor, J. W. *Int. J. Mass Spectrom. Ion Phys.* **1980**, *35*, 273.
- (2) Kebarle, P.; Haynes, R. N.; Collins, J. G. *J. Am. Chem. Soc.* **1967**, *89*, 5753.
- (3) Morgan, S.; Castleman, A. W. *J. Phys. Chem.* **1989**, *93*, 4544.
- (4) Morgan, S.; Keesee, R. G.; Castleman, A. W. *J. Am. Chem. Soc.* **1989**, *111*, 3841.
- (5) Vaidyanathan, G.; Coolbaugh, M. T.; Garvey, J. F. *J. Phys. Chem.* **1992**, *96*, 1589.
- (6) Stace, A. J.; Shukla, A. K. *J. Am. Chem. Soc.* **1982**, *104*, 5314.
- (7) Nishi, N.; Yamamoto, K. *J. Am. Chem. Soc.* **1987**, *109*, 7353.

- (8) Yang, S. F.; Brereton, S. M.; Ellis, A. M. *Int. J. Mass Spectrom.* **2006**, *253*, 79.
- (9) Hu, Y. J.; Fu, H. B.; Bernstein, E. R. *J. Chem. Phys.* **2006**, *125*, 154306.
- (10) Shi, Y. J.; Consta, S.; Das, A. K.; Mallik, B.; Lacey, D.; Lipson, R. H. *J. Chem. Phys.* **2002**, *116*, 6990.
- (11) Remacle, F.; Levine, R. D. *J. Chem. Phys.* **2006**, *125*, 133321.
- (12) Woon, D. E. *Adv. Space Res.* **2004**, *33*, 44.
- (13) Raina, G.; Kulkarni, G. U. *Chem. Phys. Lett.* **2001**, *337*, 269.
- (14) Short, L. C.; Cai, S. S.; Syage, J. A. *J. Am. Soc. Mass Spectrom.* **2007**, *18*, 589.
- (15) Garvey, J. F.; Herron, W. J.; Vaidyanathan, G. *Chem. Rev.* **1994**, *94*, 1999.
- (16) Shi, Z.; Wei, S.; Ford, J. V.; Castleman, A. W. *Chem. Phys. Lett.* **1992**, *200*, 142.
- (17) Fu, H. B.; Hu, Y. J.; Bernstein, E. R. *J. Chem. Phys.* **2006**, *124*, 024302.
- (18) Dong, F.; Heinbuch, S.; Rocca, J. J.; Bernstein, E. R. *J. Chem. Phys.* **2006**, *124*, 224319.
- (19) Wakisaka, A.; Abdoul-Carime, H.; Yamamoto, Y.; Kiyozumi, Y. *J. Chem. Soc., Faraday Trans.* **1998**, *94*, 369.
- (20) Booze, J. A.; Baer, T. *J. Chem. Phys.* **1992**, *96*, 5541.
- (21) Tomoda, S.; Kimura, K. *Chem. Phys.* **1983**, *74*, 121.
- (22) Martrenchard-Barra, S.; Gregoire, G.; Dedonder-Lardeux, C.; Jouvot, C.; Solgadi, D. *PhysChemComm* **1999**, *4*, 15.
- (23) Lee, S. Y.; Shin, D. N.; Cho, S. G.; Jung, K. H.; Jung, K. W. *J. Mass Spectrom.* **1995**, *30*, 969.
- (24) Tsai, S. T.; Jiang, J. C.; Lee, Y. T.; Kung, A. H.; Lin, S. H.; Ni, C. K. *J. Chem. Phys.* **1999**, *111*, 3434.
- (25) Belau, L.; Wilson, K. R.; Leone, S. R.; Ahmed, M. *J. Phys. Chem. A* **2007**, *111*, 10075.
- (26) Raina, G.; Kulkarni, G. U.; Rao, C. N. R. *J. Phys. Chem. A* **2001**, *105*, 10204.
- (27) McGlashan, M. L.; Williamson, A. G. *J. Chem. Eng. Data* **1976**, *21*, 196.
- (28) Morgan, S.; Castleman, A. W. *J. Am. Chem. Soc.* **1987**, *109*, 2867.
- (29) Elshall, M. S.; Marks, C.; Sieck, L. W.; Meotner, M. *J. Phys. Chem.* **1992**, *96*, 2045.
- (30) Lykтей, M. M. Y.; DeLeon, R. L.; Shores, K. S.; Furlani, T. R.; Garvey, J. F. *J. Phys. Chem. A* **2000**, *104*, 5197.
- (31) Kirschner, K. N.; Woods, R. J. *J. Phys. Chem. A* **2001**, *105*, 4150.
- (32) Harich, S. A.; Hwang, D. W. H.; Yang, X. F.; Lin, J. J.; Yang, X. M.; Dixon, R. N. *J. Chem. Phys.* **2000**, *113*, 10073.
- (33) <http://www.webbook.nist.gov>.
- (34) Tsai, S. T.; Jiang, J. C.; Lin, M. F.; Lee, Y. T.; Ni, C. K. *J. Chem. Phys.* **2004**, *120*, 8979.
- (35) Masella, M.; Flament, J. P. *J. Chem. Phys.* **1998**, *108*, 7141.
- (36) Curtiss, L. A.; Blander, M. *Chem. Rev.* **1988**, *88*, 827.
- (37) Mejia, S. M.; Espinal, J. F.; Restrepo, A.; Mondragon, F. *J. Phys. Chem. A* **2007**, *111*, 8250.
- (38) Fileti, E. E.; Chaudhuri, P.; Canuto, S. *Chem. Phys. Lett.* **2004**, *400*, 494.